THE JOURNAL OF BIOLOGICAL CHEMISTRY
Vol. 276, No. 19, Issue of May 11, pp. 15876–15880, 2001

Printed in U.S.A.

Human RAD52 Exhibits Two Modes of Self-association*

Received for publication, December 27, 2000
Published, JBC Papers in Press, February 13, 2001, DOI 10.1074/jbc.M011747200

Wasantha Ranatunga‡§, Doba Jackson‡§, Janice A. Lloyd§¶, Anthony L. Forget§¶, Kendall L. Knight¶, and Gloria E. O. Borgstahl‡‖

From the ‡Department of Chemistry, University of Toledo, Toledo, Ohio 43606-3390 and the ¶Department of Biochemistry and Molecular Pharmacology, University of Massachusetts Medical School, Worcester, Massachusetts 01655-0103

The human RAD52 protein plays an important role in the earliest stages of chromosomal double-strand break repair via the homologous recombination pathway. Individual subunits of RAD52 self-associate into rings that can then form higher order complexes. RAD52 binds to double-strand DNA ends, and recent studies suggest that the higher order self-association of the rings promotes DNA end-joining. Earlier studies defined the self-association domain of RAD52 to a unique region in the N-terminal half of the protein. Here we show that there are in fact two experimentally separable self-association domains in RAD52. The N-terminal self-association domain mediates the assembly of monomers into rings, and the previously unidentified domain in the C-terminal half of the protein mediates higher order self-association of the rings.

The repair of double-strand breaks in chromosomal DNA is of critical importance for the maintenance of genomic integrity. In *Saccharomyces cerevisiae*, genes of the *RAD52* epistasis group, *RAD50*, *RAD51*, *RAD52*, *RAD54*, *RAD55*, *RAD57*, *RAD59*, *MRE11*, and *XRS2*, were identified initially by the sensitivity of mutants to ionizing radiation (1, 2). These genes have been implicated in an array of recombination events including mitotic and meiotic recombination as well as double-strand break repair. *RAD52* mutants show the most severe pleiotropic defects suggesting a critical role for the protein in homologous recombination and double-strand break repair (2). The importance of specific protein-protein interactions in the catalysis of homologous recombination is suggested by studies demonstrating specific contacts and functional interactions between Rad52p and a number of proteins involved in recombination including Rad51p (3–8), which catalyzes homologous pairing and strand exchange, and replication factor A (RPA)[1] (8–10), a heterotrimeric single-stranded DNA binding protein (11).

Studies of the equivalent human proteins have identified similar interactions between the RAD52, RAD51, and replication protein A proteins (12–17). Based on a series of protein-protein interaction assays (15, 16, 18) and DNA binding studies[2] (16), a domain map of RAD52 was proposed by Park *et al.* (16) (see Fig. 1). The determinants of self-association were proposed to exist exclusively within a region defined by residues 65–165, a result supported by recent studies of several isoforms of RAD52 (19). Electron microscopy (EM) studies of Rad52p and RAD52 have revealed formation of ring-shaped structures (9–13 nm in diameter), as well as higher order aggregates (9, 12, 20). Stasiak *et al.* (21) performed image analyses of negatively stained electron micrographs and determined that the 10-nm RAD52 rings are composed of seven subunits. Scanning transmission electron microscopy (STEM) analysis indicated a mean mass of 330 ± 59 kDa supporting a heptameric ring-shaped RAD52 structure (21). Recent studies show that RAD52 binds to double-stranded DNA ends as an aggregated complex (20). These end-binding complexes were amorphous in shape and ranged in size from 15 to 60 nm. Within these complexes, RAD52 rings were observed occasionally. Binding of RAD52 to the DNA ends promoted end-to-end association between DNA molecules and stimulated ligation of both cohesive and blunt DNA ends (20).

Therefore, given that the formation of both ring-shaped oligomers and aggregates of these rings seem relevant to RAD52 function, we sought to investigate further the self-association properties of the RAD52 protein. We performed a series of analyses comparing full-length RAD52-(1–418) with two different mutant RAD52 proteins: (i) a 1–192 mutant that spans the N-terminal portion and includes the entire proposed DNA binding and self-association domains and (ii) a 218–418 mutant that spans the C-terminal portion of RAD52 that includes the proposed RPA- and RAD51-binding domains (Fig. 1). In contrast to previous studies, our results show that there are experimentally separable determinants for two different modes of self-association by RAD52, one in the N-terminal and one in the C-terminal portion of the protein.

EXPERIMENTAL PROCEDURES

RAD52 Constructs—Wild-type *RAD52* and *RAD52*-(1–192) pET28 expression plasmids were a gift from Dr. M. Park and have six histidines fused to the C terminus. A pET28 expression plasmid containing the thioredoxin-RAD52-(218–418) fusion protein was constructed using standard polymerase chain reaction techniques.

Protein Purification—Cultures of transformed BL21(DE3) Codon Plus *Escherichia coli* (Stratagene) were grown in a fermentor and induced with 0.5 mM isopropyl-1-thio-β-D-galactopyranoside. Wild-type *RAD52* and *RAD52*-(1–192) cells were resuspended in a buffer consisting of 20 mM HEPES, pH 6.0, 10% glycerol, 400 mM NaCl, 100 mM KCl, 5 mM β-mercaptoethanol, 1 mM dithiothreitol, 1 mM hexylglucopyranoside, and 1 mM EDTA. *RAD52*-(218–418) cells were resuspended in a

* This work was supported by the United States Army Medical Research and Material Command under DAMD17-98-1-8251 (to G. E. O. B.) and National Institutes of Health Grant GM44772 (to K. L. K.). Brookhaven National Laboratory STEM is supported by National Institutes of Health Grant P41-RR01777 and partially supported by the Department of Energy and Office of Biological and Environmental Research. The costs of publication of this article were defrayed in part by the payment of page charges. This article must therefore be hereby marked "*advertisement*" in accordance with 18 U.S.C. Section 1734 solely to indicate this fact.

§ These authors contributed equally to this work.
‖ To whom correspondence should be addressed: Dept. of Chemistry, University of Toledo, 2801 W. Bancroft St., Toledo, OH 43606-3390. Tel.: 419-530-1501; Fax: 419-530-4033; E-mail: gborgst@uoft02.utoledo.edu.

[1] The abbreviations used are: RPA, replication protein A; MES, 4-morpholineethanesulfonic acid; EM, electron microscopy; STEM, scanning transmission electron microscopy; BSA, bovine serum albumin; DLS, dynamic light scattering.

[2] J. A. Lloyd, and K. L. Knight, unpublished data.

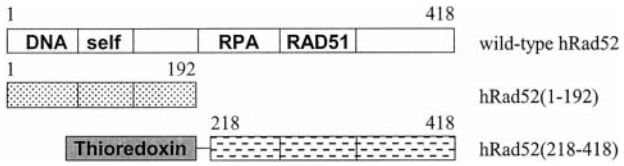

FIG. 1. **Schematic diagram of wild-type RAD52 and deletion mutants.** The beginning and ending residue numbers of each mutant are indicated along with domain structure. The following domains and residue numbers were defined by Park *et al.* (16): DNA binding, 39–80; self-association, 85–159; RPA binding, 221–280; RAD51 binding, 290–330.

buffer consisting of 50 mM HEPES, pH 8, 500 mM KCl, 500 mM $LiSO_4$, 2.5% glycerol, 1 mM EDTA, 5 mM dithiothreitol, 4 mM imidazole, and 0.1% Triton X-100. Protease inhibitors (1 mM phenylmethylsulfonyl fluoride and 10 mM benzamidine) were used throughout purification. Cells were lysed using a French press, and the lysate was clarified by centrifugation, filtration through Cell Debris Remover-modified cellulose (Whatman), and passage through a 0.22-μm pore filter. The clarified lysate was applied to an MC/M Ni^{2+} affinity column (PerSeptive Biosystems) that was optimally washed and eluted with an imidazole gradient. Wild-type RAD52 and RAD52-(1–192) then were dialyzed extensively against a buffer consisting of 20 mM MES, pH 6.0, 10% glycerol, 400 mM NaCl, 100 mM KCl, 5 mM β-mercaptoethanol, 1 mM dithiothreitol, 1 mM hexylglucopyranoside, and 1 mM EDTA. RAD52-(218–418) was dialyzed extensively against a buffer consisting of 50 mM HEPES, pH 8.0, 2.5% glycerol, 2.5 mM EDTA, and 0.5 mM hexylglucopyranoside and then purified further by anion exchange using an HQ/M column (PerSeptive Biosystems) eluted with a KCl gradient. Protein samples were concentrated using Amicon concentrators with YM10 membranes, and protein concentrations were determined using Bradford assay (Bio-Rad) with bovine serum albumin (BSA) as a standard. The expression plasmid for wild-type RPA heterotrimer was a gift from Dr. M. Wold. RPA was expressed and purified as described (22).

Enzyme-linked Immunosorbent Assay—The enzyme-linked immunosorbent assay was done at room temperature. Briefly, 10 pmol of wild-type RAD52, RAD52 mutants, or BSA were coated to microtiter plates for 1 h. Plates were washed three times with phosphate-buffered saline (PBS) containing 0.02% Tween 20 to remove unbound protein. Plates then were blocked with 5% milk in PBS for 10 min and then washed. Various amounts of RPA in PBS and 5% milk were added and incubated for 1 h. Plates then were washed to remove nonspecific interactions and probed with a monoclonal antibody against the 70-kDa subunit of RPA (Calbiochem) in PBS and 5% milk for 30 min. Plates then were washed and probed with anti-mouse IgG peroxidase conjugate (Sigma) in PBS and 5% milk for 30 min and washed. Plates were developed using 3,3′,5,5′-tetramethylbenzidine in phosphate-citrate buffer with 0.03% hydrogen peroxide. Color was developed for 30 min, the reaction was stopped with 1.5 M H_2SO_4, and absorbance readings at 450 nm were taken with a microtiter plate reader. Background absorbance was determined from a blank well and then subtracted from the data.

Gel-shift DNA Binding Assays—Reactions (20 μl) contained 20 mM triethanolamine-HCl, pH 7.5, 1 mM dithiothreitol, 1 mM $MgCl_2$, 0.1 mg/ml BSA, 0.05% Tween 20, 2 nM 5′-end-labeled 95 base oligonucleotide (concentration in bases), and the indicated amounts of protein. The oligonucleotide sequence is as follows: 5′-AGA CGA TAG CGA AGG CGT AGC AGA AAC TAA CGA AGA TTT TGG CGG TGG TCT GAA CGA CAT CTT TGA GGC GCA GAA AAT CGA GTG GCA CTA ATA AG-3′. Reactions were incubated at 37 °C for 20 min followed by the addition of glutaraldehyde to 0.2% and continued incubation at 22 °C for 20 min. Glycerol was added to a final concentration of 1.6% (w/v) and samples (10 μl) were loaded onto a 0.8% agarose gel and electrophoresed at 100 mV in 0.5× TBE buffer (90 mM Tris, 64.6 mM boric acid, and 2.5 mM EDTA, pH 8.3). Gels were analyzed using a Molecular Imager FX and QuantityOne software (Bio-Rad). The 95-base oligonucleotide used in the gel-shift assays was made using an ABI 392 DNA/RNA synthesizer.

Dynamic Light-scattering (DLS) Analysis—DLS was carried out using a DynaPro-801 molecular sizing instrument equipped with a microsampler (Protein Solutions). A 50-μl sample was passed through a filtering assembly into a 12-μl chamber quartz cuvette. For RAD52-(1–192) and RAD52-(218–418), 20-nm filters were used. For wild-type RAD52, a 100-nm filter was used. The data were analyzed first using Dynamics 4.0 software and then DynaLS software as follows. Hydrodynamic radii (R_H) for monomodal distributions, as defined by a baseline ranging from 0.977 to 1.002, were reported from Dynamics 4.0. Bi- and multimodal distributions were analyzed using DynaLS. DynaLS data estimates of molecular weight were obtained from R_H using Dynamics 3.0 molecular weight calculator. Sum of squares errors less than 5000 were considered negligible.

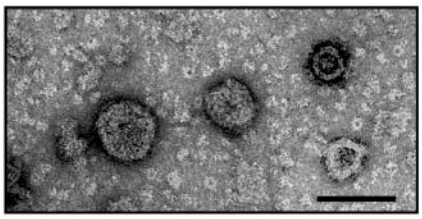

FIG. 2. **Negative stained electron micrograph of wild-type RAD52.** Wild-type RAD52 (4.0 μM) was prepared as described under "Experimental Procedures." Larger spherical particles are ~80 nm in diameter, half-spheres are 50 nm, and numerous 10-nm rings are visible also. *Black bar* = 0.1 μm.

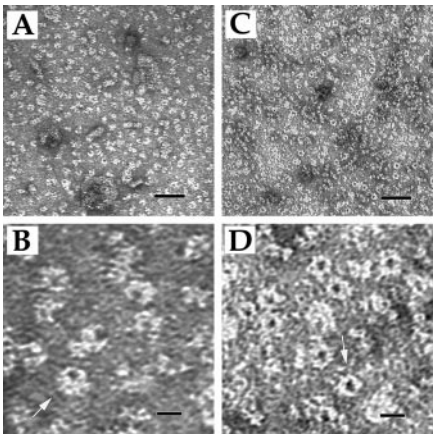

FIG. 3. **Negative stained electron micrographs of wild-type RAD52 and RAD52-(1–192) protein.** Proteins (4.0 μM) were prepared as described under "Experimental Procedures." The majority of protein for both wild-type RAD52 (*A* and *B*) and RAD52-(1–192) (*C* and *D*) forms 10-nm diameter ring-shaped oligomers. Larger particles of wild-type RAD52 in *A* (also see Fig. 2) are not formed by RAD52-(1–192). Higher magnifications of both proteins reveal that the protrusions observed on the 10-nm rings of wild-type RAD52 are missing in the RAD52-(1–192) rings (*arrows* in *B* and *D*). *Black bars* = 0.05 μm in *A* and *C* and 0.01 μm in *B* and *D*.

Electron Microscopy—Proteins were prepared for EM by diluting wild-type or mutant RAD52 to 4.0 μM in a buffer containing 20 mM Tris-HCl, pH 7.5, 5% glycerol, 5 mM β-mercaptoethanol, 0.1 mM EDTA, and 100 mM KCl. Samples were spread onto thin carbon films on holey carbon grids (400 mesh), stained with 1% uranyl acetate, and visualized by transmission electron microscopy using a Philips CM10 microscope.

STEM Analysis—Analyses were carried out at the Brookhaven National Laboratory using unstained, unshadowed freeze-dried samples. Protein samples (~0.1 mg/ml) were applied to a thin carbon film supported by a thick holey film on titanium grids and freeze-dried overnight. The microscope operates at 40 kV. Operation of the STEM and data analyses were performed as described previously (23).

Gel Filtration—Samples of the RAD52-(218–418) protein at 1.2 mg/ml were loaded onto a Superdex 200 HR 10/30 gel filtration column (Amersham Pharmacia Biotech/LKB) equilibrated in buffer containing 20 mM MES, pH 6.0, 400 mM NaCl, 100 mM KCl, 10% (w/v) glycerol, 5 mM β-mercaptoethanol, and 1 mM EDTA. Analysis was performed using a BioLogic chromatography system (Bio-Rad) with an in-line UV detector.

RESULTS

Oligomeric Characteristics of RAD52 Proteins—EM analyses of wild-type RAD52 and RAD52-(1–192) show that both proteins form ring-shaped structures (Figs. 2 and 3). The average diameter of these particles, measured across the surface with the central pore, is 10 ± 1 nm, consistent with previous reports (9, 12, 21). Wild-type RAD52 also forms distinct larger particles that appear as various sized spheres and half-spheres ranging in diameter from 30 to 100 nm (Fig. 2). These particles consist of individual 10-nm rings as well as other less distinct com-

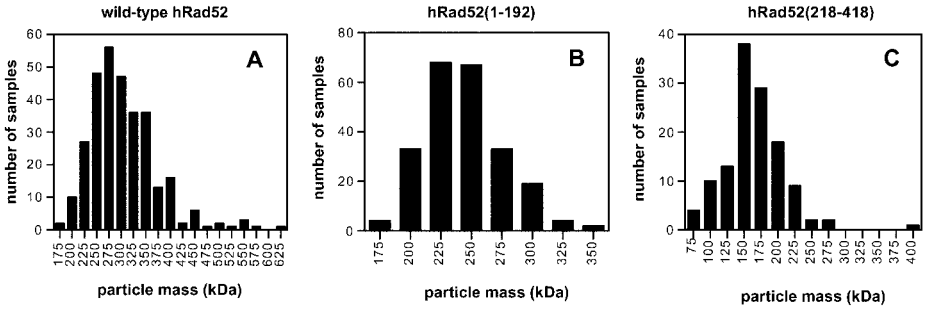

FIG. 4. **STEM histograms.** STEM mass analyses were performed as described under "Experimental Procedures." Histograms include pooled data from several separate analyses (eight for wild-type RAD52, six for RAD52-(1–192), and five for RAD52-(218–418)). Average mass values were as follows: *A*, wild-type RAD52 298 ± 69 kDa (n = 309); *B*, RAD52-(1–192) 227 ± 30 kDa (n = 277); *C*, RAD52-(218–418) 153 ± 40 kDa (n = 119).

TABLE I
Dynamic light-scattering measurements of RAD52 proteins

Protein	Concentration	Base line	Modality	SOS[a]	R_H[b]	Molecular mass	Peak[c] area
	mg/ml			*error*	*nm*	*kDa*	*%*
RAD52	3.5	1.007	Multimodal	3.10	6.6 (0.7)	279	10.5
					27.6 (9.3)	9.05×10^3	85.8
					711.0 (245)	2.40×10^7	3.7
RAD52-(1–192)	15	1.001	Monomodal	1.95	5.7 (1.2)	200	
RAD52-(218–418)	2	1.001	Monomodal	0.64	4.6 (2.1)	118	
Thioredoxin	1	1.001	Monomodal	3.3	2.0 (0.8)	14.8	

[a] SOS, sum of squares.
[b] Average hydrodynamic radius (R_H) is reported with the polydispersity (width of the distribution in nm) given in parentheses.
[c] For DynaLS results the percent peak area for the solvent peak is not reported.

pressed structures. For RAD52-(1–192) the majority of protein forms ring-shaped oligomers, and no larger particles were seen (Fig. 3). Even at increased concentrations (6 and 10 μM) RAD52-(1–192) shows no larger aggregates (data not shown). Higher magnifications reveal "protrusions" extending from the 10-nm rings formed by wild-type RAD52 that are missing in the 1–192 protein (see *arrows* in Fig. 3, *B* and *D*). These protrusions likely correspond to those modeled by Stasiak *et al.* (21), and our data show that they are part of the C-terminal portion of RAD52.

STEM analyses of wild-type RAD52 (2 μM) showed particle sizes ranging from 175 to 625 kDa with a mass average of 298 ± 69 kDa (n = 309; Fig. 4*A*). Given a molecular mass of 48 kDa for the His-tagged RAD52 protein, this range corresponds to particles that contain from 4 to 13 subunits with an average of six subunits. Similar analyses of the 1–192 protein showed particle sizes ranging from 100 to 350 kDa with a mass average of 227 ± 30 kDa (n = 277; Fig. 4*B*). For a monomer molecular mass of 23 kDa, this range corresponds to particles that contain from 4 to 15 subunits with an average of 10 subunits. Resolution of the ring-shaped oligomers in the electron micrographs was not high enough to count individual subunits, but our STEM data are consistent with previous work in which oligomeric rings of wild-type RAD52 were determined to be heptameric (21).

The oligomeric distribution of these proteins in solution was investigated by DLS. Wild-type RAD52 shows a multimodal profile with three peaks corresponding to particles with an average hydrodynamic radius of 6.6, 27.6, and 711.0 nm, respectively (Table I). These likely correspond to ring-shaped oligomers, the 30-nm particles described previously as "super-rings" (12) and seen in our micrographs (Fig. 2), and larger aggregates also observed in our micrographs. We find that the percent distribution of these various sized particles is effected by protein concentration, *i.e.* with increasing concentration the larger aggregates account for a larger percentage of the population. In contrast to wild type, RAD52-(1–192) shows a monomodal light-scattering profile that corresponds to a particle with a hydrodynamic radius of 6.1 nm (Table I), which is in agreement with our EM analysis.

The above analyses indicate at least two modes of RAD52 self-association that are experimentally separable, (i) formation of ring-shaped oligomers and (ii) formation of larger aggregates. Because the latter seems to depend largely on the presence of residues C-terminal to position 192, we performed a number of assays to test for self-association on a mutant RAD52 containing only residues 218–418. Initial EM studies showed no distinct structural characteristics for this protein (data not shown), but STEM analysis revealed particle sizes ranging from 75 to 275 kDa (Fig. 4*C*) with a mass average of 153 ± 40 kDa (n = 119; Fig. 4*C*). Given a monomer molecular mass of 39 kDa, the particle composition ranges from two to seven subunits with an average of four subunits. Gel filtration shows a homogeneous peak corresponding to a molecular mass of 166 kDa (Fig. 5) and therefore to a particle containing approximately four subunits. Analysis by DLS shows a monomodal peak corresponding to a particle with an average R_H of 4.6 nm and a molecular mass of 118 kDa (therefore containing approximately three subunits). DLS measurements on thioredoxin alone show that it does not contribute to the oligomeric character of thioredoxin-RAD52-(218–418) (Table I). Together,

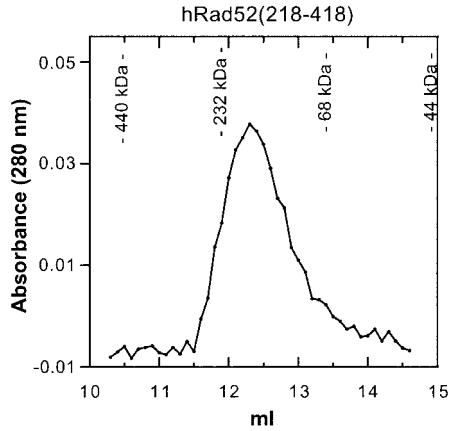

FIG. 5. **Gel filtration profile of the thioredoxin/218–418 fusion RAD52 protein.** The mutant protein (1.2 mg/ml, 35.8 μM) was loaded onto a Superdex 200 HR 10/30 gel filtration column, and elution of protein was followed at $A_{280\ nm}$. The indicated elution volumes of standards (ferritin, *440 kDa*; catalase, *232 kDa*; BSA, *68 kDa*; ovalbumin, *44 kDa*) were an average of four runs.

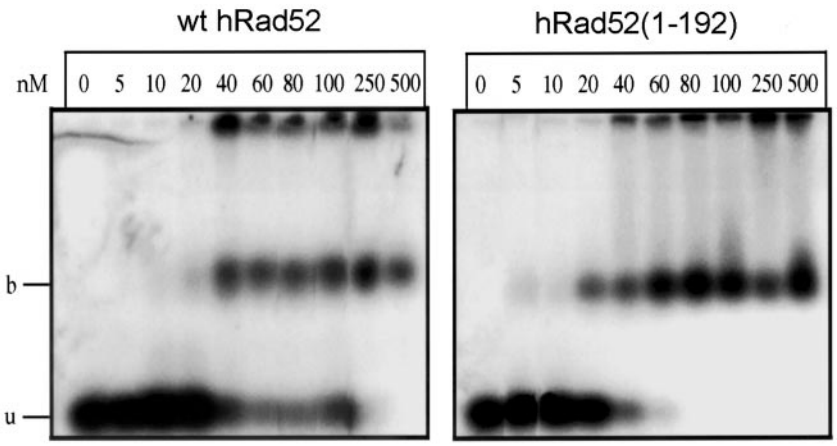

FIG. 6. **Gel-shift DNA Binding assays.** Indicated concentrations of either wild-type RAD52 or RAD52-(1–192) were incubated with a 5′-end-labeled 95-base oligonucleotide followed by cross-linking with glutaraldehyde as described under "Experimental Procedures." Reactions were electrophoresed on a 0.8% agarose gel. Radioactive material at the *top* of the gel represents protein-DNA complex trapped in the gel well. *u*, unbound DNA; *b*, protein-DNA complex.

these data indicate that the C-terminal portion of RAD52 (residues 218–418) contains determinants of protein self-association that are distinct from those required to form 10-nm rings.

DNA Binding—Binding of wild-type RAD52 and RAD52-(1–192) to single-stranded DNA was analyzed by gel-shift assays. The gels in Fig. 6 are representative of five different experiments, each of which gave similar results. In each case, analysis of unbound and bound DNA (including that in the gel well) gave rise to a $K_{D(app)}$ of 35 and 25 nM for wild-type RAD52 and RAD52-(1–192), respectively. This slight enhancement in binding affinity was observed consistently for RAD52-(1–192). With wild-type RAD52 a significant portion of bound DNA remained in the gel well, a result that likely reflects the ability of the wild-type protein to form greater amounts of self-aggregates than the 1–192 mutant protein (see below). Additionally, 100% of the DNA (2 nM total nucleotides) was bound by the 1–192 protein at 40–60 nM protein in the titration profile, whereas 100% binding by wild-type RAD52 consistently required greater than 100 nM protein. Assays using the RAD52-(218–418) mutant protein showed no DNA binding up to 2.0 μM protein (data not shown). These results show that the DNA binding domain of RAD52 is contained within the N-terminal portion of the protein and that removal of the C-terminal 227 residues results in a slight enhancement of DNA binding.

Interaction of RAD52 Proteins with RPA—Previous studies have mapped residues 221–280 as the domain in RAD52 that interacts with the 32-kDa subunit of RPA (16). To ensure that the 218–418 mutant construct maintained a native fold, we tested this protein for interaction with RPA using an immunoassay. Enzyme-linked immunosorbent assays showed that the 218–418 protein interacted with RPA with an affinity similar to that observed for wild-type RAD52 (Fig. 7). No interaction with RPA was observed for RAD52-(1–192), thioredoxin, or BSA.

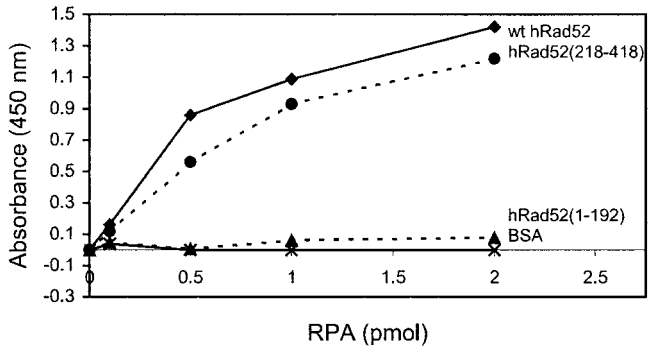

FIG. 7. **RAD52-RPA protein-protein interactions.** Enzyme-linked immunosorbent assays were performed as described under "Experimental Procedures" with RAD52 proteins immobilized to microtiter plates and probed with increasing amounts of RPA heterotrimer. The experiment was performed in triplicate, and the average for each RPA concentration was plotted. The error was on the order of 5–10%. *wt*, wild type.

DISCUSSION

Previous studies have shown that RAD52 exists in a number of oligomeric states ranging from rings with a 10-nm diameter to larger complexes with diameters of greater than 30 nm (9, 12, 20, 21). Recent observations indicate a direct role for these higher order protein-protein interactions in promoting DNA end-joining (20). We therefore sought to investigate the self-association properties of RAD52 utilizing an array of biophysical techniques.

In our EM studies of wild-type RAD52 and RAD52-(1–192), we observed ring structures with an average diameter of 10 ± 1 nm as has been reported previously (9, 12, 20, 21). Additionally, and as seen previously (12, 20, 21), we observed protrusions extending from wild-type RAD52 rings as well as a population of distinct larger particles. However, neither the protrusions nor the larger particles were observed with RAD52-(1–192). This suggests that residues within the C-terminal portion of the protein (residues 193–418) make up these protrusions and carry determinants for higher order RAD52 self-association.

DLS analysis of wild-type RAD52 and the two mutant proteins provides additional and complementary evidence for two distinct modes of RAD52 self-association. DLS analysis of wild-type RAD52 shows three peaks that likely correspond to the 10-nm ring-shaped oligomers and the 30-nm and larger particles observed by EM. In contrast, both RAD52-(1–192) and RAD52-(218–418) show a monomodal DLS profile indicating the presence of a single population of structures. The RAD52-(1–192) R_H is consistent with a ring structure, and the RAD52-(218–418) R_H indicates a complex composed of three subunits. This self-association of RAD52-(218–418) was confirmed by size-exclusion chromatography and STEM.

The ability of RAD52-(218–418) to self-associate was unexpected. Previous studies have suggested that residues 65–165 define the exclusive self-association domain in the RAD52 protein (18). Shen *et al.* (18) found that although N-terminal fragments of the protein self-associated in two-hybrid screens and affinity chromatography assays, fragments containing various portions of the C terminus, *e.g.* 287–418 or 166–418, did not. In contrast to these results, we find that RAD52-(218–418) is able to self-associate. Although our EM analysis revealed no distinct oligomeric structures for RAD52-(218–418), three different methods (STEM, gel filtration, and DLS) showed that this mutant formed oligomeric particles containing 3–4 subunits. These data for RAD52-(218–418), coupled with the inability of RAD52-(1–192) to form structures larger than the 10-nm rings, indicate that residues within the C-terminal region of the pro-

tein make important contributions to RAD52 self-association. Thus, the C-terminal region of RAD52 contains a novel self-association domain distinct from that previously identified within residues 65–165 (18).

Importantly, functional analyses of both the 1–192 and 218–418 mutant proteins show that each maintains an expected activity. Both wild-type RAD52 and the 1–192 proteins, which form ring-shaped oligomers, bound single-stranded DNA with similar affinities. This is consistent with previous studies that mapped the DNA binding domain of RAD52 to residues 39–80[2] (16). The elevated affinity of RAD52-(1–192) for single-stranded DNA was noted also for a similar Rad52p construct (24). Also as expected, RAD52-(218–418) showed a specific interaction with RPA. Again, this is consistent with previous studies that mapped the RPA interaction domain to residues 221–280 in RAD52 (16). The fact that both mutant proteins showed the expected functions demonstrates that they very likely maintain native structure, thereby supporting the relevance of differences observed in their oligomeric characteristics compared with wild-type RAD52.

In summary, our data support a model in which the self-association domain within the N-terminal region of RAD52 (residues 1–192) promotes the formation of ring-shaped oligomers that are functional for DNA binding, whereas the C-terminal domain (residues 218–418) mediates higher order self-association events. Additionally, the protrusions extending from the 10-nm ring structure of wild-type RAD52, originally modeled by Stasiak *et al.* (21) and seen clearly in our electron micrographs, correspond to the C-terminal region of the protein. Given the likely importance of higher order self-association to the ability of RAD52 to promote end-to-end joining of DNA breaks (20), these protrusions seem to mediate a critically important aspect of RAD52 function. Further studies of various mutant RAD52 proteins will clarify the contribution made by the different aspects of self-association toward the overall function of this important DNA repair protein.

Acknowledgments—We thank Matt Pokross and Jeff Habel for technical assistance and Krishnamurthy Rajeswari and Cathy Schellert for help in the early stages of this project. We also thank Dr. Min Park at Los Alamos National Laboratory for wild-type *RAD52* and *RAD52*-(1–192) expression plasmids. We gratefully acknowledge Dr. Martha Simon at Brookhaven National Laboratory for performing the STEM analyses.

REFERENCES

1. Game, J., and Mortimer, R. K. (1974) *Mutat. Res.* **24,** 281–292
2. Petes, T. D., Malone, R. E., and Symington, L. S. (1991) in *The Molecular and Cellular Biology of the Yeast, Saccharomyces* (Broach, J. R., Pringle, J. R., and Jones, E. W., eds) pp. 407–522, Cold Spring Harbor Laboratory Press, Cold Spring Harbor, NY
3. Shinohara, A., and Ogawa, T. (1998) *Nature* **391,** 404–407
4. Milne, G. T., and Weaver, D. T. (1993) *Genes Dev.* **7,** 1755–1765
5. Hays, S. L., Firmenich, A. A., and Berg, P. (1995) *Proc. Natl. Acad. Sci., U. S. A.* **92,** 6925–6929
6. Johnson, R. D., and Symington, L. S. (1995) *Mol. Cell. Biol.* **15,** 4843–4850
7. Sung, P. (1997) *J. Biol. Chem.* **272,** 28194–28197
8. New, J. H., Sugiyama, T., Zaitseva, E., and Kowalczykowski, S. C. (1998) *Nature* **391,** 407–410
9. Shinohara, A., Shinohara, M., Ohta, T., Matsuda, S., and Ogawa, T. (1998) *Genes Cells* **3,** 145–156
10. Sugiyama, T., New, J. H., and Kowalczykowski, S. C. (1998) *Proc. Natl. Acad. Sci. U. S. A.* **95,** 6049–6054
11. Wold, M. S. (1997) *Annu. Rev. Biochem.* **66,** 61–91
12. Van Dyck, E., Hajibagheri, N. M. A., Stasiak, A., and West, S. C. (1998) *J. Mol. Biol.* **284,** 1027–1038
13. Golub, E. I., Gupta, R. C., Haaf, T., Wold, M. S., and Radding, C. M. (1998) *Nucleic Acids Res.* **26,** 5388–5393
14. Baumann, P., and West, S. C. (1999) *J. Mol. Biol.* **291,** 363–374
15. Shen, Z., Cloud, K. G., Chen, D. J., and Park, M. S. (1996) *J. Biol. Chem.* **271,** 148–152
16. Park, M. S., Ludwig, D. L., Stigger, E., and Lee, S. H. (1996) *J. Biol. Chem.* **271,** 18996–19000
17. Benson, F. E., Baumann, P., and West, S. C. (1998) *Nature* **391,** 401–404
18. Shen, Z., Peterson, S. R., Comeaux, J. C., Zastrow, D., Moyzis, R. K., Bradbury, E. M., and Chen, D. J. (1996) *Mutat. Res.* **364,** 81–89
19. Kito, K., Wada, H., Yeh, E. T., and Kamitani, T. (1999) *Biochim. Biophys. Acta* **1489,** 303–314
20. Van Dyck, E., Stasiak, A. Z., Stasiak, A., and West, S. C. (1999) *Nature* **398,** 728–731
21. Stasiak, A. Z., Larquet, E., Stasiak, A., Muller, S., Engel, A., Dyck, E. V., West, S. C., and Egelman, E. H. (2000) *Curr. Biol.* **10,** 337–340
22. Henricksen, L. A., Umbricht, C. B., and Wold, M. S. (1994) *J. Biol. Chem.* **269,** 11121–11132
23. Wall, J. S., Hainfeld, J. F., and Simon, M. N. (1998) *Methods Cell Biol.* **53,** 139–164
24. Mortensen, U. H., Bendixen, C., Sunjevaric, I., and Rothstein, R. (1996) *Proc. Natl. Acad. Sci. U. S. A.* **93,** 10729–10734